

Cyclic spin exchange in cuprate spin ladders

Tamara S. Nunner,¹ Philipp Brune,² Thilo Kopp,¹ Marco Windt,³ and Markus Grüninger³

¹*EP VI, Universität Augsburg, 86135 Augsburg, Germany*

²*TP III, Universität Augsburg, 86135 Augsburg, Germany*

³*II. Physikalisches Institut, Universität zu Köln, 50937 Köln, Germany*

(Received 22 March 2002; published 27 November 2002)

We investigate the influence of a cyclic spin exchange J_{cyc} on the one- and two-triplet excitations of an undoped two-leg $S=1/2$ ladder, using the density-matrix renormalization group (DMRG). The dispersion of the $S=0$ two-triplet bound state is dramatically reduced by J_{cyc} due to a repulsion between triplets on neighboring rungs. In $(\text{La,Ca})_{14}\text{Cu}_{24}\text{O}_{41}$ a consistent description of both the spin gap and the $S=0$ bound state requires $J_{cyc}/J_{\perp} \approx 0.20-0.27$ and $J/J_{\perp} \approx 1.25-1.35$. With these coupling ratios the recently developed dynamical DMRG yields an excellent description of the entire $S=0$ excitation spectrum observed in the optical conductivity, including the continuum contribution.

DOI: 10.1103/PhysRevB.66.180404

PACS number(s): 75.10.Jm, 75.30.Et, 75.40.Gb, 75.40.Mg

The antiferromagnetic parent compounds of the high- T_c cuprates are thought to be the best representatives of the two-dimensional $S=1/2$ square-lattice Heisenberg model. Understanding their magnetic properties is of utmost importance due to the intimate relationship of magnetic correlations and high- T_c superconductivity. Recently, the question of how to set up a minimal model which accounts for these magnetic properties has been readdressed. High-resolution inelastic-neutron-scattering experiments performed on the two-dimensional $S=1/2$ antiferromagnet La_2CuO_4 exhibit a magnon dispersion at the zone boundary,¹ which cannot be obtained within a nearest-neighbor Heisenberg model. It has been argued that the inclusion of a cyclic spin-exchange term of about 20% would reproduce this dispersion.² This cyclic spin exchange emerges as a correction to the nearest-neighbor Heisenberg Hamiltonian of order t^4/U^3 from a t/U expansion of the one-band Hubbard model.³ It is expected to be the dominant correction within a more realistic three-band description of the CuO_2 planes, because there the cyclic permutation of four spins on a plaquette can take place without double occupancy.^{4,5} Similar cyclic spin-exchange processes have proven to be significant in other systems, e.g., in cuprate spin chains a ferromagnetic two-spin cyclic exchange is responsible for the unusually strong exchange anisotropy.⁶

Cuprate spin ladders offer an alternative approach to decide about the existence and potential implications of a cyclic spin-exchange term. They are composed of the same corner-sharing Cu-O plaquettes as the two-dimensional cuprates, thus similar exchange couplings are expected for all spin products. In fact the inclusion of a cyclic spin exchange has been suggested in order to explain the smallness of the ladder spin gap observed in $(\text{La,Ca})_{14}\text{Cu}_{24}\text{O}_{41}$.⁷⁻⁹ However, it is impossible to extract a unique set of coupling parameters or even to settle the existence of a cyclic spin-exchange term from an analysis of the spin gap only. Here, the optical conductivity^{10,11} $\sigma(\omega)$ can provide the missing information because dynamic quantities are expected to be influenced by additional four-spin interactions^{12,13} as suggested in Ref. 13 for the two-dimensional cuprates. Magnetic excitations can be observed in $\sigma(\omega)$ via the simultaneous excitation of a

phonon.^{14,15} In $(\text{La,Ca})_{14}\text{Cu}_{24}\text{O}_{41}$, two peaks in $\sigma(\omega)$ were identified as $S=0$ bound states of two triplets.¹⁰

Here we show that a consistent evaluation of $\sigma(\omega)$ is achieved by the inclusion of J_{cyc} . The dispersion of the $S=0$ bound state is very sensitive to the magnitude of J_{cyc} . The combined analysis of both the $S=0$ bound state and the spin gap establishes a unique set of exchange couplings, namely, $J_{cyc}/J_{\perp} \approx 0.20-0.27$, $J/J_{\perp} \approx 1.25-1.35$, and $J_{\perp} = 950-1100 \text{ cm}^{-1}$ for $(\text{La,Ca})_{14}\text{Cu}_{24}\text{O}_{41}$. For these values, we calculate the entire spectrum of $\sigma(\omega)$ using the dynamical density-matrix renormalization group (DMRG),¹⁶ and find excellent agreement with new experimental data, which yield an improved estimate of the continuum contribution. This clearly confirms the above value for J_{cyc} . One might speculate that such a sizable cyclic spin-exchange term will have significant consequences for superconductivity in the doped spin ladders,¹⁷ since magnetic and pairing correlations are considered as closely related phenomena.¹⁸

We study an isolated two-leg $S=1/2$ ladder characterized by an antiferromagnetic Heisenberg Hamiltonian with an additional cyclic spin-exchange term:

$$\begin{aligned}
 H = & J_{\perp} \sum_i \mathbf{S}_{i,l} \mathbf{S}_{i,r} + J \sum_i (\mathbf{S}_{i,l} \mathbf{S}_{i+1,l} + \mathbf{S}_{i,r} \mathbf{S}_{i+1,r}) \\
 & + J_{cyc} \sum_i \frac{1}{4} (P_{(i,l)(i,r)(i+1,r)(i+1,l)} \\
 & + P_{(i,l)(i,r)(i+1,r)(i+1,l)}^{-1}), \quad (1)
 \end{aligned}$$

where J_{\perp} and J denote the rung and leg couplings, the index i refers to the rungs, and l, r label the two legs. The cyclic permutation operator P_{1234} for four spins on a plaquette is given by

$$\begin{aligned}
 P_{1234} + P_{1234}^{-1} \\
 = & 4(\mathbf{S}_1 \mathbf{S}_2)(\mathbf{S}_3 \mathbf{S}_4) + 4(\mathbf{S}_1 \mathbf{S}_4)(\mathbf{S}_2 \mathbf{S}_3) - 4(\mathbf{S}_1 \mathbf{S}_3)(\mathbf{S}_2 \mathbf{S}_4) \\
 & + \mathbf{S}_1 \mathbf{S}_2 + \mathbf{S}_3 \mathbf{S}_4 + \mathbf{S}_1 \mathbf{S}_4 + \mathbf{S}_2 \mathbf{S}_3 + \mathbf{S}_1 \mathbf{S}_3 + \mathbf{S}_2 \mathbf{S}_4. \quad (2)
 \end{aligned}$$

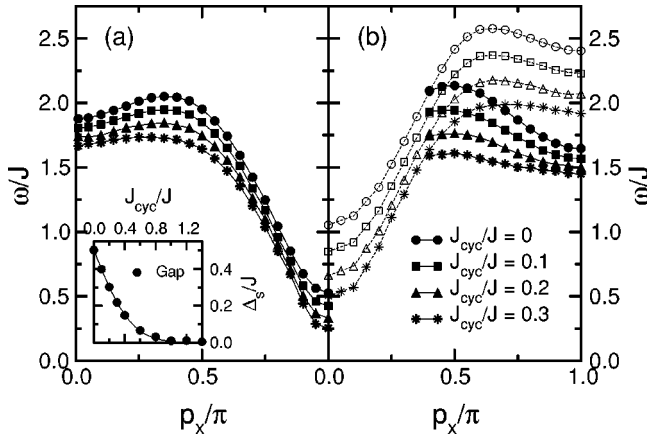


FIG. 1. DMRG results for an $N=80$ site ladder with $J=J_{\perp}$ and $0 \leq J_{cyc}/J \leq 0.3$. (a) One-triplet dispersion (corresponds to $p_y = \pi$ of the spin-spin correlation function). The inset shows the spin gap Δ_s [extrapolated to $N=\infty$ (Ref. 23)] as a function of J_{cyc}/J . (b) Lower edge of the two-triplet continuum (corresponds to $p_y=0$ of the spin-spin correlation function, open symbols) and the $S=0$ two-triplet bound state (full symbols). The bound state is obtained as the pole of $\langle\langle \delta B_{-p}^{leg}; \delta B_p^{leg} \rangle\rangle$, which is explicitly given below Eq. (4).

The influence of J_{cyc} can easily be understood in terms of the representation of the spin operators by rung singlets s_i^{\dagger} and triplets $t_{i,\alpha}^{\dagger}$ ($\alpha=x,y,z$):^{19,20}

$$\begin{aligned}
 H = \sum_i & \left\{ \frac{9}{16} J_{cyc} - \frac{3}{4} (J_{\perp} + \frac{1}{2} J_{cyc}) s_i^{\dagger} s_i \right. \\
 & + \frac{1}{4} (J_{\perp} - \frac{11}{2} J_{cyc}) \sum_{\alpha} t_{i,\alpha}^{\dagger} t_{i,\alpha} \\
 & + \frac{1}{2} (J + \frac{1}{2} J_{cyc}) \sum_{\alpha} [s_i^{\dagger} s_{i+1} t_{i+1,\alpha}^{\dagger} t_{i,\alpha} + \text{H.c.}] \\
 & + \frac{1}{2} (J - \frac{1}{2} J_{cyc}) \sum_{\alpha} [s_i^{\dagger} s_{i+1}^{\dagger} t_{i+1,\alpha} t_{i,\alpha} + \text{H.c.}] \\
 & + \frac{1}{4} (J + \frac{1}{2} J_{cyc}) \sum_{\alpha,\beta} (1 - \delta_{\alpha\beta}) \\
 & \times [t_{i,\alpha}^{\dagger} t_{i+1,\beta}^{\dagger} t_{i+1,\alpha} t_{i,\beta} - t_{i,\alpha}^{\dagger} t_{i+1,\alpha}^{\dagger} t_{i+1,\beta} t_{i,\beta} + \text{H.c.}] \\
 & \left. + J_{cyc} \sum_{\alpha,\beta} t_{i,\alpha}^{\dagger} t_{i,\alpha} t_{i+1,\beta}^{\dagger} t_{i+1,\beta} \right\}. \quad (3)
 \end{aligned}$$

The consideration of J_{cyc} primarily renormalizes the coupling strengths of the individual terms in the original Heisenberg Hamiltonian. The only new contribution is the last term, a repulsive interaction between triplets on neighboring rungs. With respect to the renormalization of the coupling constants, the strongest effect is a reduction of the triplet bond energy. Consequently the spin gap as well as the energy of the entire one-triplet dispersion are reduced. In Fig. 1(a) we show the one-triplet dispersion, obtained by the Lanczos-vector method^{21,22} for an $N=80$ site ladder with $J=J_{\perp}$ and different values of J_{cyc} . The shape of the one-triplet dispersion remains qualitatively unchanged. The strongest suppres-

sion affects the minimum ($p_x = \pi$) and the maximum (near $p_x \approx \pi/3$). Nevertheless, there still is a local minimum at $p_x=0$ even for $J_{cyc}/J=0.3$, in contrast to the exact diagonalization results for a $N=24$ site ladder in Ref. 7. Extrapolating to an infinite ladder,²³ we find that the spin gap $\Delta_s = E_0(N=\infty, S=1) - E_0(N=\infty, S=0)$ decreases rapidly [inset of Fig. 1(a)], in agreement with Ref. 25.

Similar considerations also apply to the two-triplet excitations. With increasing J_{cyc} , the lower edge of the two-triplet continuum [open symbols in Fig. 1(b)] shifts corresponding to the one-triplet dispersion. In addition, however, a repulsive interaction between neighboring triplets is introduced by J_{cyc} , as mentioned above [see Eq. (3)]. This reduces the binding energy of the $S=0$ two-triplet bound state. As a consequence the width of the bound-state dispersion decreases dramatically [full symbols in Fig. 1(b)]. Evidently the dispersion of the $S=0$ two-triplet bound state is very sensitive to the magnitude of J_{cyc} and thus provides a suitable quantity to probe the existence and magnitude of a cyclic spin exchange.

In $(\text{La,Ca})_{14}\text{Cu}_{24}\text{O}_{41}$ the $S=0$ bound state has been observed in the optical conductivity $\sigma(\omega)$ via phonon-assisted two-triplet absorption.¹⁰ Although the total momentum of the excitation has to be zero, the simultaneous excitation of a phonon with arbitrary momentum permits to measure a weighted average of the $S=0$ excitations from the entire Brillouin zone. In Fig. 3 we show the magnetic contribution to $\sigma(\omega)$ in $\text{La}_{5.2}\text{Ca}_{8.8}\text{Cu}_{24}\text{O}_{41}$.²⁶ For polarization of the electrical field parallel to the legs, the two peaks in $\sigma_{leg}(\omega)$ at $\omega_1 = 2140 \text{ cm}^{-1}$ and $\omega_2 = 2780 \text{ cm}^{-1}$ correspond to van Hove singularities resulting from the maximum ω_{max} and minimum ω_{min} of the $S=0$ bound-state dispersion at $p_x \approx \pi/2$ and $p_x = \pi$, respectively [see Fig. 1(b)]. The broad features at higher energies represent the continuum contribution.

In order to determine the exchange couplings for $\text{La}_{5.2}\text{Ca}_{8.8}\text{Cu}_{24}\text{O}_{41}$ we have calculated ω_{max} and ω_{min} for different coupling ratios J/J_{\perp} and J_{cyc}/J_{\perp} using the Lanczos-vector method.²² By extrapolation to an infinite ladder²³ we obtain the values displayed in Fig. 2(a). The corresponding results for the spin gap Δ_s are shown in Fig. 2(b). In the range depicted in Fig. 2 these values may be approximated within 5% by $\omega_{min} \approx 1.64J_{\perp} - 0.54J_{cyc}$, $\omega_{max} \approx 0.61J_{\perp} - 1.87J_{cyc} + 1.53J$, and $\Delta_s \approx 0.48J_{\perp} - 0.84J_{cyc}$. In principle, the three experimental quantities ω_1 , ω_2 , and $\Delta_s \approx 280 \text{ cm}^{-1}$ (Ref. 8) should suffice to determine J_{cyc} , J , and J_{\perp} . However, ω_1 and ω_2 depend also on the frequency ω_{ph} of the phonon involved in the optical absorption process, i.e., $\omega_1 = \omega_{min} + \omega_{ph}^{p_x=\pi}$ and $\omega_2 = \omega_{max} + \omega_{ph}^{p_x=\pi/2}$. Making use of the relative insensitivity of Δ_s and ω_{min} on J/J_{\perp} (see Fig. 2) we can determine the magnitude of the cyclic spin exchange without the consideration of ω_2 and hence omit any effect of a possible phonon dispersion. For a conservative estimate of the Cu-O bond-stretching phonon frequency $\omega_{ph}^{p_x=\pi} = 600 \pm 100 \text{ cm}^{-1}$, we obtain $J_{cyc}/J_{\perp} = 0.20 - 0.27$ with $J_{\perp} \approx 950 - 1100 \text{ cm}^{-1}$. The dispersion of the phonon enters only

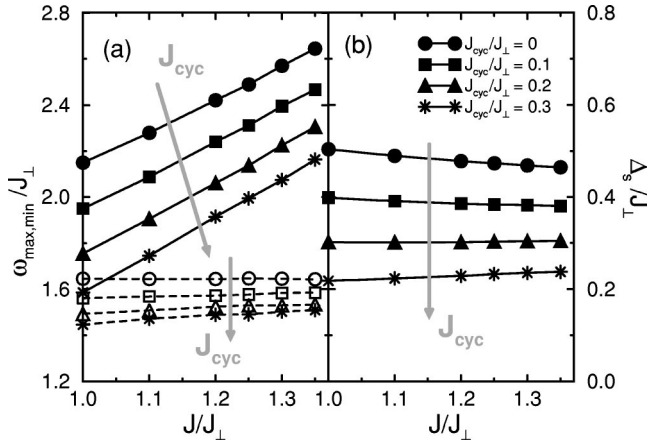


FIG. 2. (a) Maximum of the $S=0$ bound-state dispersion at $p_x \approx \pi/2$ (full symbols), minimum at $p_x = \pi$ (open symbols) and (b) spin gap Δ_s as a function of J/J_\perp for different values of J_{cyc}/J_\perp . All results have been extrapolated to $N = \infty$ (Ref. 23).

in the determination of the coupling ratio J/J_\perp . Allowing for a dispersion of $\omega_{ph}^{p_x=\pi/2} - \omega_{ph}^{p_x=\pi} \approx \pm 50 \text{ cm}^{-1}$ (Ref. 30) we obtain $J/J_\perp \approx 1.25-1.35$.

Up to now we have derived a set of exchange couplings which consistently describes the spin gap and the $S=0$ two-triplet bound state. Now we compare the spectral density

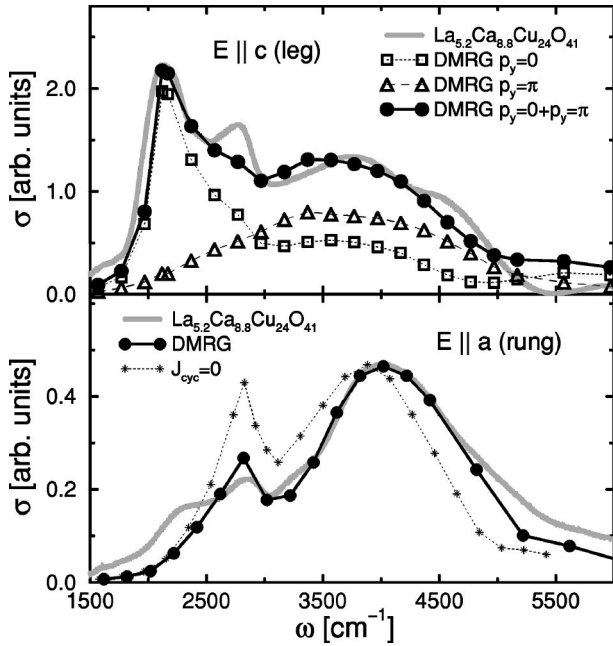


FIG. 3. Symbols: Correction-vector results for the optical conductivity $\sigma(\omega)$ of an $N=80$ site ladder with polarization of the electrical field E along the legs (top panel) and along the rungs (bottom panel), using $J/J_\perp = 1.3$, $J_{cyc}/J_\perp = 0.2$, $J_\perp = 1000 \text{ cm}^{-1}$, $\omega_{ph}^{\text{leg}} = 570 \text{ cm}^{-1}$, $\omega_{ph}^{\text{rung}} = 620 \text{ cm}^{-1}$ (Ref. 30) and a finite broadening of $\delta = 0.1J_\perp$. The leg polarization contains two contributions, where the two legs are in-phase ($p_y=0$) or out-of-phase ($p_y=\pi$) with each other. Gray lines: $\sigma(\omega)$ of $\text{La}_{5.2}\text{Ca}_{8.8}\text{Cu}_{24}\text{O}_{41}$ at $T=4 \text{ K}$ (Ref. 26). Stars (bottom panel): fit for $J_{cyc}=0$ with $J/J_\perp = 1.15$, $J_\perp = 960 \text{ cm}^{-1}$, $\omega_{ph}^{\text{rung}} = 620 \text{ cm}^{-1}$.

calculated for this parameter set with the line shape of the entire spectrum observed in $\sigma(\omega)$. This provides a thorough test of whether we indeed have found the minimal model that captures all relevant properties. We consider an isolated Cu_2O_3 ladder, for which the major contribution to $\sigma(\omega)$ results from the simultaneous excitation of two neighboring spin flips plus a Cu-O bond-stretching phonon:

$$\sigma(\omega) \sim -\omega \sum_{p_x} \sum_{p_y=0,\pi} f_p \text{Im} \langle \langle \delta B_{-p}; \delta B_p \rangle \rangle_{(\omega-\omega_{ph})}, \quad (4)$$

where $\delta B_p^{\text{leg}} = (1/N) \sum_i \sum_{k=l,r} e^{ipr_{i,k}} (\mathbf{S}_{i,k} \mathbf{S}_{i+1,k} - \langle \mathbf{S}_{i,k} \mathbf{S}_{i+1,k} \rangle)$ and $\delta B_p^{\text{rung}} = (1/N) \sum_i e^{ipr_i} (\mathbf{S}_{i,l} \mathbf{S}_{i,r} - \langle \mathbf{S}_{i,l} \mathbf{S}_{i,r} \rangle)$ are the spin-flip operators for polarization of the electrical field along the legs and the rungs, respectively. To lowest order (fourth order in the Cu-O hopping t_{pd}), the dominant contribution to the phonon form factor f_p^{leg} comes from the in-phase and the out-of-phase stretching modes of the O ions on the legs, whereas for f_p^{rung} the out-of-phase stretching mode and the vibration of the O ion on the rung are taken into account (Ref. 27):

$$f_p^{\text{leg}} = 8 \sin^4\left(\frac{p_x}{2}\right), \quad f_p^{\text{rung}} = 8 \sin^2\left(\frac{p_x}{2}\right) + 4. \quad (5)$$

So far we have used the Lanczos-vector method²¹ (LVM) to calculate the dispersion of the bound state. This was justified by the fact that the LVM uses the first Lanczos vectors as target states besides the ground state, and consequently represents the bound state quite accurately. However, in order to calculate the high-frequency range of $\sigma(\omega)$ the LVM is not reliable. We use the correction-vector method,^{16,28} because here the density matrix is optimized to represent the correction vector for each frequency point separately.

In Fig. 3 we compare $\sigma(\omega)$ for polarization along the legs and along the rungs, obtained by the correction-vector method for a ladder with $N=80$ sites, with the experimental result of $\text{La}_{5.2}\text{Ca}_{8.8}\text{Cu}_{24}\text{O}_{41}$.²⁶ Here we have used $J/J_\perp = 1.3$ and $J_{cyc}/J_\perp = 0.2$ with $J_\perp = 1000 \text{ cm}^{-1}$.³⁰ For polarization along the legs, $\sigma(\omega)$ contains two contributions, where the two legs are excited in-phase ($p_y=0$) or out-of-phase ($p_y=\pi$). The in-phase mode contains two- and four-triplet excitations, as can be inferred from the rung-triplet representation of the spin-flip operator $\mathbf{S}_{i,l} \mathbf{S}_{i+1,l} + \mathbf{S}_{i,r} \mathbf{S}_{i+1,r}$ in Eq. (3). It includes the $S=0$ two-triplet bound state as discussed above. The out-of-phase mode reflects excitations of three triplets due to $\mathbf{S}_{i,l} \mathbf{S}_{i+1,l} - \mathbf{S}_{i,r} \mathbf{S}_{i+1,r} = (i/2) \sum_{\alpha,\beta,\gamma} \epsilon_{\alpha\beta\gamma} \{ t_{i,\alpha}^\dagger t_{i+1,\beta}^\dagger t_{i+1,\gamma}^\dagger + t_{i,\beta}^\dagger t_{i+1,\alpha}^\dagger t_{i+1,\gamma}^\dagger + t_{i,\gamma}^\dagger t_{i+1,\alpha}^\dagger t_{i+1,\beta}^\dagger - \text{H.c.} \}$ and hence contributes only to the high-energy continuum excitations.³¹ For polarization along the rungs, $\sigma(\omega)$ contains only two-triplet excitations [see Eq. (3) for the rung-triplet representation of $\mathbf{S}_{i,l} \mathbf{S}_{i,r}$], and the lower bound state is suppressed due to a selection rule.¹⁰

Comparing the DMRG results for polarization along the legs with the experimental spectra we find excellent agreement within the range of the bound state (which has been used in order to fix the coupling constants), and also with respect to the overall line shape of the high-energy continuum excitations. For this polarization the experimental determination of the precise spectral weight of the continuum is

difficult due to an electronic background.^{10,11,26} The small differences between experiment and theory in the continuum range are certainly within the experimental error bars. For polarization along the rungs, where experimentally the magnetic contribution to $\sigma(\omega)$ can be identified unambiguously and with high precision,^{10,11} the continuum is reproduced nearly perfectly. This provides strong evidence that a nearest-neighbor Heisenberg Hamiltonian with $J/J_{\perp}=1.3$ and an additional cyclic spin exchange of $J_{cyc}/J_{\perp}=0.2$ represent the magnetic excitations of the spin-ladder compound $(\text{La,Ca})_{14}\text{Cu}_{24}\text{O}_{41}$.

Any spectrum calculated for $J_{cyc}=0$ cannot reach the quality shown above. For $J_{cyc}=0$, the positions of the bound states can be described correctly with $J/J_{\perp}=1.09-1.19$. In the lower panel of Fig. 3 we plot the spectrum obtained for $J_{cyc}=0$ and $J/J_{\perp}=1.15$ and find a strong discrepancy with the experimental result. The weight of the bound states is too large compared to the continuum, and the energy cutoff of the continuum is too low.

In spite of the overall impressive consistency of experiment and theory, some discrepancies are visible: (i) In $\sigma_{\text{leg}}(\omega)$ the upper bound state (for $p_x \approx \pi/2$) is suppressed much stronger in the DMRG calculation than in the experimental spectrum. (ii) In $\sigma_{\text{rung}}(\omega)$ the experimental data displays a pronounced shoulder at about 2200 cm^{-1} , i.e., slightly above the suppressed lower bound state, which is not present in our DMRG calculation. We propose that these

discrepancies are related to different phonon form factors which arise due to the actual arrangement of the ladders within the trellis lattice, and in higher order (with respect to Cu-O hopping) in the external photon-electron-phonon vertex (Ref. 27). Considering, e.g., an additional term $\propto \sin^2(p_x/2)$ in f_p^{leg} will enhance the weight of the upper bound state in $\sigma_{\text{leg}}(\omega)$ with respect to the lower one. Such considerations, however, depend on the details of the nonlocal excitation process in these ladder systems and are therefore not of fundamental relevance.

In summary, we have demonstrated that the inclusion of a cyclic spin exchange J_{cyc} is necessary to obtain a consistent interpretation of optical experiments and the magnitude of the spin gap in $(\text{La,Ca})_{14}\text{Cu}_{24}\text{O}_{41}$. The dispersion of the $S=0$ bound state is very sensitive to the magnitude of J_{cyc} . Quantitative investigation yields $J_{cyc}/J_{\perp} \approx 0.20-0.27$ and $J/J_{\perp} \approx 1.25-1.35$ with $J_{\perp} \approx 950-1100 \text{ cm}^{-1}$. With these parameters we obtain excellent agreement with the experimental spectra of $\text{La}_{5.2}\text{Ca}_{8.8}\text{Cu}_{24}\text{O}_{41}$, both for the bound state and the continuum. This gives strong evidence that we indeed have identified the minimal model which captures all relevant magnetic properties.

We would like to thank M. Greiter, A. P. Kampf, and G. S. Uhrig for stimulating discussions. This project was supported by the DFG (SFB 484 and SFB 608) and by the BMBF (13N6918/1).

-
- ¹R. Coldea *et al.*, Phys. Rev. Lett. **86**, 5377 (2001).
²A.A. Katanin and A.P. Kampf, Phys. Rev. B **66**, 100403 (2002).
³A.H. MacDonald, S.M. Girvin, and D. Yoshioka, Phys. Rev. B **37**, 9753 (1988); **41**, 2565 (1990).
⁴E. Müller-Hartmann and A. Reischl, Eur. Phys. J. B **28**, 173 (2002).
⁵H.J. Schmidt and Y. Kuramoto, Physica C **167**, 263 (1990).
⁶V. Kataev *et al.*, Phys. Rev. Lett. **86**, 2882 (2001).
⁷S. Brehmer *et al.*, Phys. Rev. B **60**, 329 (1999).
⁸M. Matsuda *et al.*, Phys. Rev. B **62**, 8903 (2000); J. Appl. Phys. **87**, 6271 (2000).
⁹D.C. Johnston *et al.*, cond-mat/0001147 (unpublished).
¹⁰M. Windt *et al.*, Phys. Rev. Lett. **87**, 127002 (2001).
¹¹M. Grüninger *et al.*, J. Phys. Chem. Solids **63**, 2335 (2002).
¹²A.A. Nersisyan and A.M. Tselik, Phys. Rev. Lett. **78**, 3939 (1997).
¹³J. Lorenzana, J. Eroles, and S. Sorella, Phys. Rev. Lett. **83**, 5122 (1999).
¹⁴J. Lorenzana and G.A. Sawatzky, Phys. Rev. Lett. **74**, 1867 (1995); Phys. Rev. B **52**, 9576 (1995).
¹⁵C. Jurecka and W. Brenig, Phys. Rev. B **61**, 14 307 (2000).
¹⁶T.D. Kühner and S.R. White, Phys. Rev. B **60**, 335 (1999).
¹⁷M. Uehara *et al.*, J. Phys. Soc. Jpn. **65**, 2764 (1996).
¹⁸E. Dagotto and T.M. Rice, Science **271**, 618 (1996).
¹⁹S. Sachdev and R.N. Bhatt, Phys. Rev. B **41**, 9323 (1990); S. Gopalan, T.M. Rice, and M. Sigrist, *ibid.* **49**, 8901 (1994).
²⁰In the transformation of the cyclic term, explicit use was made of the constraint: $s_i^{\dagger} s_i + \sum_{\alpha} t_{i,\alpha}^{\dagger} t_{i,\alpha} = 1$.
²¹K.A. Hallberg, Phys. Rev. B **52**, R9827 (1995).
²²All Lanczos-vector calculations were performed with three to five iterations of the finite-lattice algorithm and a maximum of 200–300 states. Four Lanczos vectors were used as target states. All calculations were performed with open boundary conditions. A Parzen filter was used to minimize edge effects for the calculation of correlation functions.
²³For all finite-size extrapolations a polynomial in $1/N$ was used, where the $1/N$ term was excluded. This is the correct finite-size scaling for the $S=1$ chain (Ref. 24).
²⁴E.S. Sørensen and I. Affleck, Phys. Rev. Lett. **71**, 1633 (1993).
²⁵Y. Honda and T. Horiguchi, cond-mat/0106426 (unpublished).
²⁶The magnetic contribution to $\sigma(\omega)$ was obtained by subtracting an electronic background. In σ_{rung} , this background is small and can be identified unambiguously (Ref. 11). In σ_{leg} measurements on a thin sample ($d \approx 6 \mu\text{m}$) allowed for a considerable improvement of the background determination with respect to Refs. 10 and 11. Details will be published elsewhere.
²⁷T.S. Nunner *et al.*, in Proceedings of SCES 2002 [Acta Phys. Pol. B (to be published)].
²⁸Here Ramasesha's algorithm (Ref. 29) has been used instead of the conjugate gradient method.
²⁹S. Ramasesha, J. Comput. Chem. **11**, 545 (1990).
³⁰Experimentally, the frequency of the upper bound state ω_2 is $\approx 60 \text{ cm}^{-1}$ higher in $\sigma_{\text{rung}}(\omega)$ than in $\sigma_{\text{leg}}(\omega)$, thus two different phonon frequencies are used in Fig. 3.
³¹T. S. Nunner, P. Brune, and T. Kopp (unpublished).